Limiting Efficiency of Heterojunction Solar Cells

Antonio Martí

***Abstract*—A heterojunction solar cell consists of a p-n junction between a high-bandgap and a low-bandgap semiconductor. As the cell is made up of two different semiconductors, the fundamental question that arises is whether the limiting efficiency of the heterojunction solar cell is determined by the low-bandgap semiconductor, the high-bandgap semiconductor, some value in-between or, perhaps, even some other value exceeding the limiting efficiency of single gap solar cells. In this respect, in this paper, we demonstrate that the limiting efficiency lies in-between, without the absolute limiting efficiency of single gap solar cells being exceeded. However, in spite of this result, we find that the open-circuit voltage of heterojunction solar cells can exceed the bandgap (divided by the electron charge) of the low-bandgap semiconductor, something that is not possible in single gap solar cells.**

***Index Terms*—Heterojunctions, limiting efficiency, photovoltaics, solar cells.**

I. Introduction

FIG. 1(a) details the simplified bandgap diagram of a heterojunction solar cell in which we have chosen the p semiconductor to be that with the high-bandgap (E_H) and the n semiconductor to be the one with the low-bandgap (E_L) in this example. The light from the sun is received first by the high-bandgap semiconductor and the low-bandgap semiconductor has a back reflector. The analysis we will develop here can also be easily carried out if we make the high-bandgap semiconductor n-type and the low-bandgap semiconductor p-type, in which the results are the same.

Many of today's high-efficiency solar cells are, in fact, heterojunction solar cells [1]: amorphous silicon/crystalline silicon heterojunction (with a record efficiency [2] of 26% with spectrum ASTM G-173-03 global); ZnO/CIGS [3], [4] (22.9%); CdSe/CdTe [5], [6] (22.1%); ZnCdSe/CZTS [7] (9%). The limiting efficiency of these solar cells has been implicitly assumed to be the one corresponding to the lowest bandgap material (silicon, CIGS, CdTe, CTZS in the examples enumerated) but …why not the one of the highest? Perhaps their limiting efficiency lies in-between the one with the highest bandgap semiconductor and the one with the lowest? Surprisingly, and contrarily to the case of homo-junction single-gap solar cells and tandem solar cells [8], [9] the limiting efficiency of heterojunction solar cells has not yet been discussed. This paper aims to fill this gap.

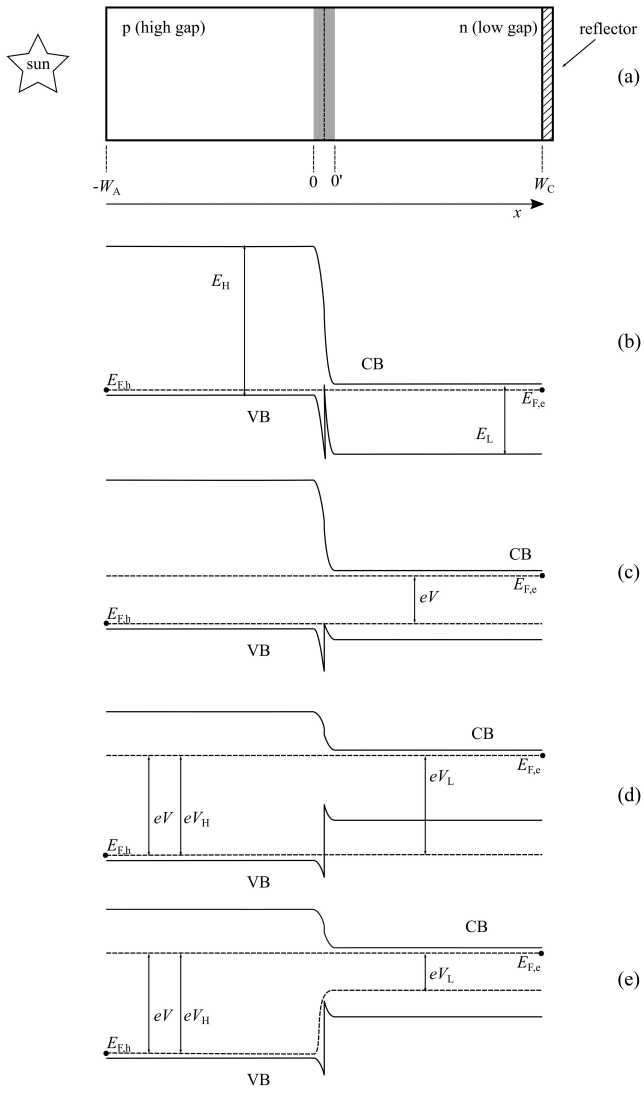

Fig. 1. (a) Structure of a heterojunction solar cell. (b) Simplified energy band diagram in equilibrium. (c) Biased at moderated voltage assuming infinite mobility. (d) Biased at high voltage under the hypothesis that the electron and hole quasi-Fermi levels remain flat. (e) Biased at high voltage under the hypothesis that mobility for the holes is finite in the transition layer.

II. Ideal Model

The basis of the theory for calculating the limiting efficiency of homo-junction single gap solar cells—or single-gap solar

Manuscript received April 22, 2019; revised July 23, 2019; accepted July 28, 2019. Date of publication August 20, 2019; date of current version October 28, 2019. This work was supported in part by the Project 2GAPS (TEC2017-92301-EXP) funded by the Spanish Ministerio de Ciencia, Innovación y Universidades, in part by the Project MADRID-PV2-CM (P2018/EMT-4308) funded by the Comunidad de Madrid supported with FEDER funds, and in part by the Project GRECO under Grant 787289 H2020, funded by the European Commission, that ensures this work is aligned to the European Open Science Policy.

The author is with the Instituto de Energía Solar of the Universidad Politécnica de Madrid, Escuela Técnica Superior de Ingenieros de Telecomunicación, Madrid 28040, Spain (e-mail: amarti@etsit.upm.es).

Color versions of one or more of the figures in this paper are available online at http://ieeexplore.ieee.org.

Digital Object Identifier 10.1109/JPHOTOV.2019.2932626

cells for short—was established by Shockley and Queisser (S&Q) in 1961 [10]. This theory establishes, on the one hand, that photons with energy below the bandgap of the semiconductor cannot be absorbed; this sets a limit to the maximum photocurrent that the cell can offer. On the other hand, after some refinements to be taken into account for stimulated emission [11], the theory also establishes that the open-circuit voltage of the solar cell cannot exceed the gap of the semiconductor (divided by the electron charge) that the cell is made of. However, a heterojunction solar cell, made up of the junction of a high-bandgap semiconductor and a low-bandgap semiconductor could plausibly provide a photo-current limited by the semiconductor with the lowest bandgap and a voltage limited by the semiconductor with the highest bandgap having, therefore, the potential to overcome S&Q efficiency limit of single-gap solar cells. We discuss next whether this is, in fact, possible or not. In our discussion, for short, when a single-gap solar cell with gap E_G appears, we will refer to the S&Q limiting efficiency of this cell as the "E_G solar cell S&Q efficiency limit." We will also clarify whether a back reflector has been placed at the back of the cell or a medium of refraction index n_r since the limiting efficiencies, for the same bandgap, are different [12].

Fig. 1 also details the band structure of a heterojunction solar cell under different biasing conditions. At the interface between both semiconductors, some characteristic spikes appear in the band diagrams that will not play any role in our discussion since, in our idealized model, it will be assumed that electrons will pass through these spikes with no difficulty.

The diagram in Fig. 1(b) illustrates the heterojunction solar cell in equilibrium and that, in Fig. 1(c), when it has been biased with a "moderate" voltage V. The mathematical model we use to calculate the limiting efficiency of the heterojunction solar cell is detailed in the Appendix. Following the same assumptions as in the S&Q detailed balance, our model assumes that the only existing electron-hole pair generation-recombination mechanism is radiative (that is, it involves the absorption or emission of a photon) and that electron and hole mobility (μ_e and μ_h, respectively) approach infinity. This last assumption is the one that leads us to draw the electron and hole quasi-Fermi levels ($E_{F,e}$ and $E_{F,h}$, respectively) in Fig. 1(c) as flat. In this respect, it will be remembered that they become flat because the electron and hole current densities, J_e and J_h, are related to the quasi-Fermi level slope through

$$J_e = \mu_e n \frac{dE_{F,e}}{dx} \tag{1}$$

$$J_e = \mu_h p \frac{dE_{F,h}}{dx} \tag{2}$$

and, therefore, $\frac{dE_{F,(e,h)}}{dx} \mapsto 0$ when $\mu_{(e,h)} \to \infty$.

If we allow for the output voltage V to increase further, we might plausibly think that we could reach a situation, as detailed in Fig. 1(d), in which the output voltage of the cell, determined by the difference between the electron and hole quasi-Fermi levels at the contacts (located at W_C and $-W_A$, respectively)

$$eV = E_{F,e}(W_C) - E_{F,h}(-W_A) \tag{3}$$

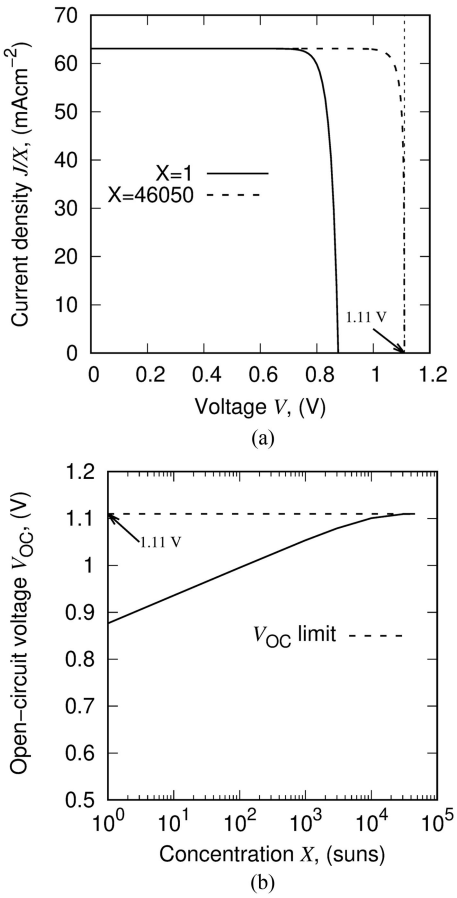

Fig. 2. (a) Current–voltage characteristic of a heterojunction solar cell characterized by $E_L = 1.11$ eV and $E_H > E_L$ for light concentrations $X = 1$ and $X = 46050$ suns. (b) Open-circuit voltage as a function of the concentration showing that it does not exceed E_L/e. In this example, the sun has been assumed as a black body at 6000 K. The cell is assumed at 300 K. The value of E_H does not impact the calculations.

could exceed the low-gap E_L. If this were the case, the limiting efficiency of a heterojunction solar cell might exceed the one of a single-gap solar cell since photon absorption and, therefore, the photocurrent would still be given determined by a low-gap E_L.

However, the situation represented in Fig. 1(d) is not physically possible because it would imply a split in the quasi-Fermi levels in the low gap semiconductor eV_L larger than the gap E_L. This situation, as anticipated before and due to the "-1" factor (see the Appendix) would result in a tremendous stimulated photon emission originated in the low-gap semiconductor that would prevent the quasi-Fermi level split eV_L from actually approaching the gap E_L.

As an illustration of this fact, Fig. 2(a) shows the current–voltage characteristic of a heterojunction solar cell characterized by $E_L = 1.11$ eV at one sun ($X = 1$) and at a maximum concentration ($X = 46050$) calculated by taking stimulated emission into account. The reason for choosing a gap of 1.11 eV in the example is that this is the optimum gap for obtaining the maximum efficiency with a single gap solar cell at this maximum concentration. As can be seen [see Fig. 2(b)], the

open-circuit voltage of the heterojunction solar cell saturates at 1.11 V without this value being exceeded. Furthermore, the model described in the Appendix shows that, due to the radiative coupling between the high-bandgap semiconductor and the low-bandgap one, the current–voltage characteristic of the cell is independent of our choice for the high-bandgap semiconductor as long as $E_H > E_L$. In other words, the performance of the heterojunction cell is identical to a cell with gap E_L and, therefore, its limiting efficiency is the same as the E_L S&Q limiting efficiency with back reflector.

III. Finite Mobility Case

The situation changes if we remove the condition of infinite carrier mobility. In this respect, Fig. 1(e) details the energy band diagram and quasi-Fermi level distribution for a case in which we assume that hole mobility is finite in a transition region at the interface between the high- and low-bandgap semiconductors (we keep the assumption of infinity electron mobility for simplicity). The transition layer could be the space charge region or a larger region. In our discussion, we will omit the generation and recombination of carriers taking place in this transition layer as it is also assumed in Shockley's ideal diode model [13].

The details of the model for the current–voltage characteristic of the heterojunction solar cell when the mobility is finite are also given in the Appendix where we show that the model can be represented approximately by the circuit in Fig. 3(a). Later we will clarify why this circuit is approximated but, for the moment, this circuit will be sufficient to understand the results. In the circuit, the diode D_H and the current generator J_H represent an ideal S&Q solar cell (without a back reflector but with a medium of refraction index n_r at the rear side) characterized by the gap E_H. The diode D_L and the current generator J_L represent an ideal S&Q solar cell (with back reflector) characterized by the gap E_L. The resistor R_h accounts for a voltage loss across the transition layer because of our assumption of finite hole mobility.

Fig. 3(b) illustrates, with one example, the current–voltage characteristic of a heterojunction solar cell that is obtained with this model as R_h evolves from zero to infinity. The example corresponds to a heterojunction solar cell characterized by $E_L = 1.11$ eV and $E_H = 1.70$ eV. For reference, these are the values that should be used to obtain the maximum efficiency for a tandem solar cell based on silicon [14]. The cell is assumed to operate at 300 K and be illuminated at maximum concentration $(X = 46050)$ with the radiation from the sun modeled as a black-body at 6000 K. When $R_h = 0$ the current–voltage characteristic is identical to the current–voltage characteristic of an ideal single-gap solar cell with gap E_L. This is not surprising since when $R_h = 0$, we recover the conventional S&Q detailed balance discussed in Section II and illustrated in Fig. 2(b) in which the carrier mobility was considered infinite. However, as R_h increases, the fill-factor of the cell decreases and, therefore, it does its efficiency [see Fig. 3(c)].

Contrarily to single-gap solar cells, in which the open-circuit voltage does not change in spite of the series resistance of the cell increasing, in the case of the heterojunction solar cell, the open-circuit voltage increases as R_h increases. We find then that the

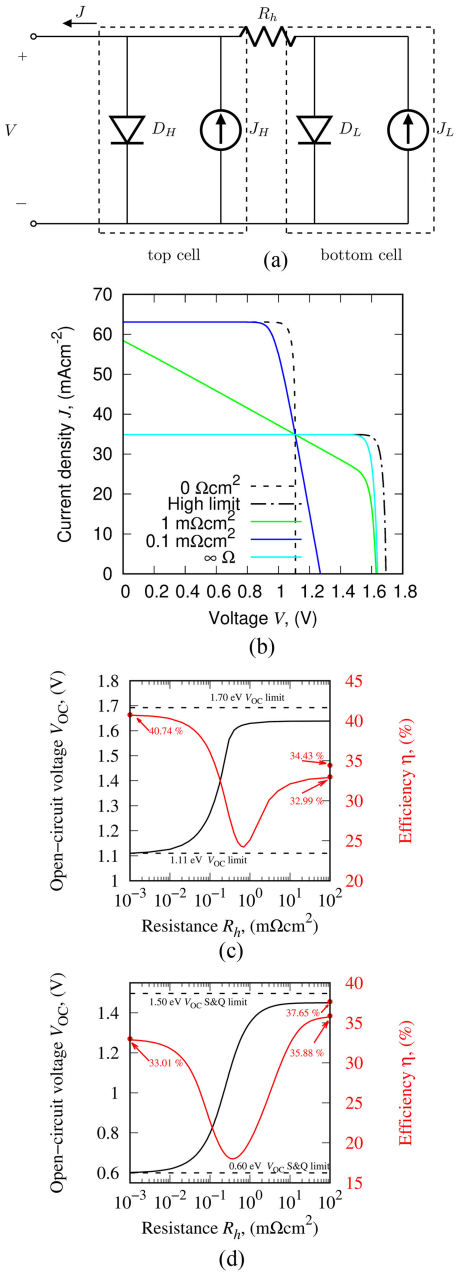

Fig. 3. (a) Simplified equivalent circuit of a heterojunction solar cell with finite carrier mobility. D_H and J_H model an ideal single-gap solar cell without a back reflector made of the high-bandgap semiconductor with $E_H = 1.7$ eV; D_L and J_L model a single-gap solar cell made of the low-bandgap semiconductor $E_L = 1.11$ eV with a back reflector. (b) Current–voltage characteristic for different values of R_h. (c) Evolution of open-circuit voltage (black line) and efficiency (red line) as the resistance R_h increases. (d) Another example of the evolution of open-circuit voltage and efficiency but for a heterojunction solar cell characterized by $E_H = 1.5$ eV and $E_L = 0.6$ eV.

open-circuit voltage of the cell exceeds the low bandgap of the heterostructure, a result that was not possible when considering homojunction single-gap solar cells. Early metal-semiconductor solar cells [15] are an example of heterostructure solar cells in which the metal can be considered as the low-bandgap semiconductor in which the gap tends toward zero (or a material in which there is no split between the electron and hole quasi-Fermi

levels). The fact that these cells demonstrated open-circuit voltages greater than zero (0.3–0.4 V) supports this result.

In fact, when $R_h \to \infty$, the open-circuit voltage (and the efficiency) of a solar cell made of the gap E_H without a back reflector is recovered. This result is easy to understand with the assistance of the circuit in Fig. 3(a) since, when $R_h \to \infty$, the cell represented by E_H ("top cell") becomes isolated from the cell represented by gap E_L ("bottom cell"). At this point it will be useful to remember that obtaining this high-output voltage has been possible without inducing an excessive high recombination because the local split of quasi-Fermi levels never exceeds the gap of the semiconductor [see Fig. 1(e)] and, therefore, the stimulated emission condition is never achieved. Hence, while in the classic S&Q detailed balance model, the output voltage of the cell and the local quasi-Fermi level split (divided by the electron charge) they were the same concept, in the heterojunction case, with finite mobility, neither concepts are equivalent.

The reason behind why the efficiency of an ideal top cell without a back reflector is recovered and not the efficiency of an ideal solar cell with a reflector is that the top cell radiates photons from the back to a media (the bottom cell) which is not a reflector but a medium of refraction index n_r (in our case we have chosen $n_r = 3.6$ as representative of a typical value for semiconductors).

Therefore, since as R_h increases the efficiency transits from the efficiency of an E_L S&Q solar cell *with* a back reflector (having chosen E_L to be the optimum gap for single-gap solar cells) to the efficiency of an E_H S&Q solar cell *without* a back reflector, we conclude that the *absolute* limiting efficiency of a heterojunction solar cell cannot exceed the limiting efficiency of a single-gap solar cell. This has not to be confused with the fact that the efficiency of the bottom cell can be exceeded if the gap of the bottom cell E_L is not optimum. This statement has been illustrated by means of Fig. 3(d) where our choice for E_L (0.6 eV) has not been the optimum one for a single-gap solar cell.

Finally, we would like to mention that our representation of the heterojunction solar cell model by means of the circuit in Fig. 3(a) has been simplified because it omits the radiative coupling between the cells. This radiative coupling, however, has been taken into account in the results shown in Fig. 3 but the simplified circuit shown in Fig. 3(a) has allowed us to discuss them more easily while maintaining the essentials of the model. The complete equivalent circuit, including the radiative coupling between the cells, can be found also in the Appendix. One of the impacts derived from considering radiative coupling is that the limiting efficiency of the heterojunction solar cell when $R_h \to \infty$ is not exactly the limiting efficiency of the top cell, considered as a single-gap solar cell with bandgap E_H without a back reflector, but slightly higher. The reason is that, when $R_h \to \infty$, the bottom cell operates in open-circuit and, under this condition, it radiates electroluminescent photons toward the top cell that are not completely monochromatic and therefore include some photons with energy $\varepsilon > E_H$ that are absorbed in the top cell improving its efficiency. However, in the examples illustrated here, the impact of this coupling is minimal since there are few electroluminescent photons with $\varepsilon > E_H$. To illustrate this with an example, we will mention that while the numerical value that we obtain for the limiting efficiency of a top cell with gap 1.70 eV without a back reflector is 32.993579864%, its limiting efficiency, when considering the luminescence from a bottom cell of 1.11 eV increases to 32.993579898% (less than 10^{-7} percentual points).

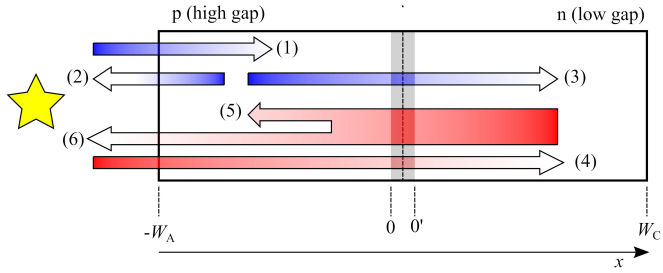

Fig. 4. Photon fluxes involved in the operation of a heterojunction solar cell working in the radiative limit: (1) $F_{\mathrm{abs},H,S} + F_{\mathrm{abs},H,\mathrm{amb}}$ represents the photons absorbed from the sun and the ambience in the high bandgap semiconductor. (2) $F_{\mathrm{em},H,F}$ represents the electroluminescent emission from the top high-bandgap semiconductor to the ambient. (3) $F_{\mathrm{abs},L,H} = F_{\mathrm{em},H,R}$ represents the electroluminescent emission from the high-bandgap semiconductor that is absorbed by the low-bandgap semiconductor. (4) $F_{\mathrm{abs},L,S} + F_{\mathrm{abs},L,\mathrm{amb}}$ represents the photons absorbed from the sun and the ambience in the low-bandgap semiconductor. (5) $F_{\mathrm{abs},H,L} = F_{\mathrm{em},L,H}$ represents the electroluminescent emission from the low-bandgap semiconductor that is absorbed in the high-bandgap semiconductor. (6) $F_{\mathrm{em},L,F}$ represents the electroluminescence emission from the low-bandgap semiconductor that escapes to the ambience.

IV. Conclusion

The absolute limiting efficiency of a heterojunction solar cell is the same as the limiting efficiency of a single-gap solar cell. A heterojunction solar cell made of a top bandgap semiconductor and a low-bandgap semiconductor will show a limiting efficiency in-between the limiting efficiency of an ideal single-gap solar cell made of the low-bandgap semiconductor and a single-gap solar cell made of the top bandgap semiconductor. The open-circuit voltage of a heterojunction solar cell can exceed the bandgap (divided by the electron charge) of the low-bandgap semiconductor if we allow for finite carrier mobility. The reason why the absolute limiting efficiency of a single gap solar cell still cannot be exceeded in spite this potential for obtaining a high open-circuit voltage is the degradation of the fill factor of the cell associated to the existence of an equivalent resistor that counts for the finite mobility of the carriers.

Appendix

For conciseness, in this appendix, we will often use the function F defined as

$$F\left(E_1, E_2, \mu, T, \Omega\right) = \frac{2\Omega}{h^3 c^2} \int_{E_1}^{E_2} \frac{y^2}{\exp \frac{y-\mu}{kT} - 1} dy. \quad (4)$$

Note, for example, that $F(0, \infty, 0, T, \pi)$ corresponds to the number of photons per unit of area and time emitted by a black body at temperature T.

Fig. 4 again represents the structure of a heterojunction solar cell together with some photon fluxes that will appear to be involved in the description of its operation.

Since the total current density J circulating across the solar cell is constant (that is, independent of x), we choose for convenience to calculate it at $x = 0$ so that

$$J = J_e(0) + J_h(0). \tag{5}$$

$J_e(0)$ being the contribution of the electron current density and $J_h(0)$ the contribution of the hole current density to the total current. We proceed first with the calculation of $J_e(0)$. To do so, by integrating the continuity equation for electrons at the p side of the heterojunction we obtain

$$\frac{1}{e}\int_{-W_A}^{0}\frac{dJ_e}{dx}dx = \int_{-W_A}^{0}(r-g)\,dx$$

$$J_e(0) - J_e(-W_A) = J_e(0) = e\int_{-W_A}^{0}(r-g)\,dx \tag{6}$$

where we have assumed that the surface at $x = -W_A$ is perfectly passivated so that $J_e(-W_A) = 0$. In (6), r is the electron-hole pair recombination rate and g the generation rate. Since we are interested in the limiting efficiency for photovoltaic conversion, we will assume that 1) only radiative recombination exists and 2) carrier mobility in the p region is infinite so that the electron and hole quasi-Fermi levels are constant. When this is the case we proved in [11] that

$$e\int_{-W_A}^{0}(r-g)\,dx = eF_{\mathrm{em},H} - eF_{\mathrm{abs},H} \tag{7}$$

where $F_{\mathrm{em},H}$ is the number of photons emitted per unit of time and unit of area and $F_{\mathrm{abs},H}$ is the number of photons absorbed per unit of time and unit of area (it is worth insisting that (7) is not valid [11] if the mobility is not infinite and, therefore, quasi-Fermi levels are not flat). The suffix "*H*" reminds us that this is a result obtained after integrating in the high-bandgap semiconductor. In our case, on the one hand

$$F_{\mathrm{em},H} = F_{\mathrm{em},H,F} + F_{\mathrm{em},H,R} \tag{8}$$

where $F_{\mathrm{em},H,F}$ is the number of photons emitted from the front side of the high-bandgap semiconductor per unit of time and area and $F_{\mathrm{em},H,R}$ is the number of photons emitted from the rear side of the high-bandgap semiconductor per unit of time and area. They are given by

$$F_{\mathrm{em},H,F} = F(E_H, \infty, eV_H, T_c, \pi) \tag{9}$$

$$F_{\mathrm{em},H,R} = n_r^2 F(E_H, \infty, eV_H, T_c, \pi) \tag{10}$$

where n_r^2 is the refraction index of the low-bandgap semiconductor (that we shall assume to be equal to the one of the high-bandgap semiconductor, for simplicity). T_C is the temperature of operation of the cell. eV_H is the split in the quasi-Fermi levels in the high-bandgap semiconductor (see Fig. 1). On the other hand

$$F_{\mathrm{abs},H} = F_{\mathrm{abs},H,S} + F_{\mathrm{abs},H,\mathrm{amb}} + F_{\mathrm{abs},H,L} \tag{11}$$

where $F_{\mathrm{abs},H,S}$ are the number of photons from the sun per unit area and time absorbed by the high-bandgap semiconductor, $F_{\mathrm{abs},H,\mathrm{amb}}$ are the number of photons from the ambience per unit area and time absorbed by the high-bandgap semiconductor, and $F_{\mathrm{abs},H,L}$ are the number of photons absorbed by the high-bandgap semiconductor coming from the electroluminescent emission of the low-bandgap semiconductor. These magnitudes are given by

$$F_{\mathrm{abs},H,S} = F(E_H, \infty, 0, T_S, H_S) \tag{12}$$

$$F_{\mathrm{abs},H,\mathrm{amb}} = F(E_H, \infty, 0, T_c, \pi - H_S) \tag{13}$$

$$F_{\mathrm{abs},H,L} = n_r^2 F(E_H, \infty, eV_L, T_c, \pi) \tag{14}$$

in which we have assumed the sun is a black body source of photons at temperature T_S, H_S is the étendue with which photons from the sun are received in the cell of unit area and that is related to the light concentration factor X by

$$H_S = \frac{X\pi}{46050} \tag{15}$$

in which $\frac{1}{46050} = \sin^2\theta_S$ where θ_s the semiangle of the sun seen from the Earth. These photon fluxes have been illustrated by means of Fig. 4.

We proceed now with the calculation of $J_h(0)$. Assuming that there is no electron-hole pair generation nor recombination at the space charge region

$$J_h(0) = J_h(0') \tag{16}$$

and $J_h(0')$ can be calculated from the hole continuity equation at the *n* low-bandgap semiconductor as

$$\frac{1}{e}\int_{0'}^{W_C}\frac{dJ_h}{dx}dx = \int_{0'}^{W_C}(g-r)\,dx$$

$$J_h(0') - J_h(W_C) = J_h(0') = e\int_{0'}^{W_C}(r-g)\,dx \tag{17}$$

where we have assumed that the surface at $x = W_C$ is perfectly passivated so that $J_h(W_C) = 0$. Similar to the case of the electrons, assuming only radiative generation-recombination at the *n* semiconductor and infinite carrier mobility we find that

$$e\int_{0'}^{W_C}(r-g)\,dx = eF_{\mathrm{em},L} - eF_{\mathrm{abs},L} \tag{18}$$

where $F_{\mathrm{em},L}$ and $F_{\mathrm{abs},L}$ are the photons emitted and absorbed per unit of area and time, respectively, by the *n* region and are given by

$$F_{\mathrm{em},L} = F_{\mathrm{em},L,H} + F_{\mathrm{em},L,F} \tag{19}$$

$$F_{\mathrm{abs},L} = F_{\mathrm{abs},L,S} + F_{\mathrm{abs},L,\mathrm{amb}} + F_{\mathrm{abs},L,H} \tag{20}$$

where per unit of time and unit of area

1) $F_{\mathrm{em},L,H}$ is the number of photons emitted by the low-gap region that are absorbed in the top high-bandgap semiconductor;
2) $F_{\mathrm{em},L,F}$ is the number of photons emitted by the low-bandgap semiconductor toward the front high-bandgap semiconductor but that are not absorbed and escape into the air because their energy is lower than the gap of the top semiconductor;
3) $F_{\mathrm{abs},L,S}$ is the number of photons from the sun absorbed by the low-bandgap semiconductor;
4) $F_{\mathrm{abs},L,\mathrm{amb}}$ is the number of photons from the ambient absorbed by the low-bandgap semiconductor;

5) $F_{\mathrm{abs},L,H} = F_{\mathrm{em},H,R}$ is the number of photons from the electroluminescent emission of the high-bandgap semiconductor absorbed by the low-bandgap semiconductor.

These magnitudes are given by

$$F_{\mathrm{em},L,H} = n_r^2 F\left(E_H, \infty, eV_L, T_C, \pi\right) \tag{21}$$

$$F_{\mathrm{em},L,F} = F\left(E_L, E_H, eV_L, T_C, \pi\right) \tag{22}$$

$$F_{\mathrm{abs},L,S} = F\left(E_L, E_H, 0, T_S, H_S\right) \tag{23}$$

$$F_{\mathrm{abs},L,\mathrm{amb}} = F\left(E_L, E_H, 0, T_C, \pi - H_S\right) \tag{24}$$

$$F_{\mathrm{abs},L,H} = n_r^2 F\left(E_H, \infty, eV_H, T_C, \pi\right). \tag{25}$$

At this point, we need a relationship between V_H and V_L. To do so, we first note that if we want to preserve our hypothesis which claims that there is no generation-recombination in the transition layer, the hole current density has to remain constant in spite of the slope of the hole quasi-Fermi level. We call this constant hole current density $\hat{J}_h$ and, across the transition layer, it has to fulfill that

$$\begin{aligned} J_h\left(0\right) &= J_h\left(0'\right) \\ &= \hat{J}_h = \mu_h p \frac{dE_{F,h}}{dx} \approx \overline{\mu_h p} \frac{E_{F,h}\left(0'\right) - E_{F,h}\left(0\right)}{\delta x} \end{aligned} \tag{26}$$

where δx is the distance between 0 and 0′. Therefore,

$$eV_H = E_{F,e} - E_{F,h}\left(0\right) = R_h \hat{J}_h + eV_L \tag{27}$$

where R_h, which has dimensions of resistance multiplied by area, is given by

$$R_h = \frac{e\delta x}{\overline{\mu_h p}}. \tag{28}$$

As a result, (5) finally results in

$$\begin{aligned} J &= J_e\left(0\right) + J_h\left(0\right) \\ &= \overbrace{F_{\mathrm{em},H,F} + F_{\mathrm{em},H,R}}^{D_H} \\ &\quad - \overbrace{F_{\mathrm{abs},H,S} + F_{\mathrm{abs},H,\mathrm{amb}}}^{J_H} \\ &\quad - \overbrace{F_{\mathrm{abs},H,L}}^{J_{CT}} + \overbrace{F_{\mathrm{em},L,H} + F_{\mathrm{em},L,F}}^{D_L} \\ &\quad - \overbrace{F_{\mathrm{abs},L,S} + F_{\mathrm{abs},L,\mathrm{amb}}}^{J_L} \\ &\quad - \overbrace{F_{\mathrm{abs},L,H}}^{J_{CB}}. \end{aligned} \tag{29}$$

Equation (28) has been represented in the circuital form in Fig. 5. The controlled current generators J_{CT} and J_{CB} count for the radiative coupling between the cells. When this coupling is neglected, we obtain the circuit shown in Fig. 3(a) in the main manuscript which was used to understand the results more easily. It has to be noted that when $E_H \equiv E_L$ and $R_h = 0$, the circuit in Fig. 5 becomes that of an ideal single gap solar cell as it could not be otherwise for the self-consistence of the model.

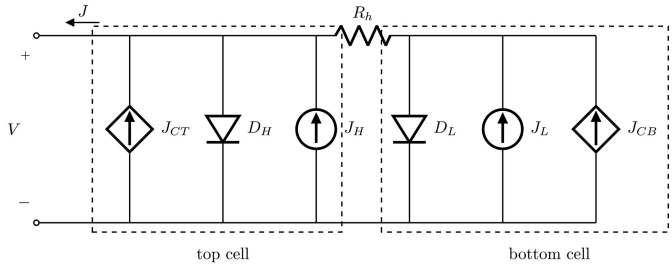

Fig. 5. Circuit model of a heterojunction solar cell taking into account radiative coupling and finite mobility.

Finally, we would like to point out that the transition layer that causes the appearance of the resistance R_h could be engineered in practice by means of an *n* layer made of a high-bandgap material. In this high-bandgap *n* layer, $p \to 0$ and, therefore, $R_h \to \infty$ [(28)].

REFERENCES

[1] M. A. Green *et al.*, "Solar cell efficiency tables (version 52)," *Prog. Photovolt. Res. Appl.*, vol. 26, no. 7, pp. 427–436, 2018.

[2] K. Yoshikawa *et al.*, "Silicon heterojunction solar cell with interdigitated back contacts for a photoconversion efficiency over 26%," *Nature Energy*, vol. 2, no. 5, pp. 17032–17032, May 2017.

[3] T. Kato, J.-L. Wu, Y. Hirai, H. Sugimoto, and V. Bermudez, "Record efficiency for thin-film polycrystalline solar cells up to 22.9% achieved by Cs-treated Cu(In,Ga)(Se,S)$_2$," *IEEE J. Photovolt.*, vol. 9, no. 1, pp. 325–330, Jan. 2019.

[4] T. Kato, "Cu(In,Ga)(Se,S)$_2$ solar cell research in Solar Frontier: Progress and current status," *Jpn. J. Appl. Phys.*, vol. 56, no. 4, 2017, Paper 04CA02.

[5] S. Krum, "First solar achieves yet another cell conversion efficiency world record | business wire," *Business Wire*, Feb. 2016. [Online]. Available: https://www.businesswire.com/news/home/20160223005315/en/. Accessed on: Jan 25, 2019.

[6] J. Britt and C. Ferekides, "Thin-film CdS/CdTe solar cell with 15.8% efficiency," *Appl. Phys. Lett.*, vol. 62, no. 22, pp. 2851–2852, May 1993.

[7] K. Sun *et al.*, "Over 9% efficient kesterite Cu_2ZnSnS_4 solar cell fabricated by using $Zn_{1-x}Cd_xS$ buffer layer," *Adv. Energy Mater.*, vol. 6, no. 12, pp. 4–9, 2016.

[8] A. Martí and G. L. Araújo, "Limiting efficiencies for photovoltaic energy conversion in multigap systems," *Sol. Energy Mater. Sol. Cells*, vol. 43, no. 2, pp. 203–222, Sep. 1996.

[9] S. Kurtz, D. Myers, W. E. McMahon, J. Geisz, and M. Steiner, "A comparison of theoretical efficiencies of multi-junction concentrator solar cells," *Prog. Photovolt. Res. Appl.*, vol. 16, no. 6, pp. 537–546, Sep. 2008.

[10] W. Shockley and H. J. Queisser, "Detailed balance limit of efficiency of p-n junction solar cells," *J. Appl. Phys.*, vol. 32, no. 3, pp. 510–519, Mar. 1961.

[11] G. L. Araújo and A. Martí, "Absolute limiting efficiencies for photovoltaic energy conversion," *Sol. Energy Mater. Sol. Cells*, vol. 33, no. 2, pp. 213–240, Jun. 1994.

[12] A. Martí, J. L. Balenzategui, and R. F. Reyna, "Photon recycling and shockley's diode equation," *J. Appl. Phys.*, vol. 82, no. 8, pp. 4067–4075, Oct. 1997.

[13] W. Shockley, "The theory of p-n junctions in semiconductors and p-n junction transistors," *Bell Syst. Tech. J.*, vol. 28, no. 3, pp. 435–489, 1949.

[14] Z. (Jason) Yu, M. Leilaeioun, and Z. Holman, "Selecting tandem partners for silicon solar cells," *Nature Energy*, vol. 1, Sep. 2016, Art. no. 16137.

[15] D. R. Lillington and W. G. Townsend, "Effects of interfacial oxide layers on the performance of silicon Schottky-barrier solar cells," *Appl. Phys. Lett.*, vol. 28, no. 2, pp. 97–98, 1976.